Design And Construction of a Sailing Winch Simulator

Patrick Campbell
MechEng MEng

2004

Supervisor:
Dr A McLaren

Abstract

This report outlines the design process, production techniques and testing procedures for a sailing winch simulator. Numerical theory is discussed and evaluated to determine whether it is relevant to a sailing winch simulator, which has been designed and constructed in order to investigate the forces on a sailing winch. The design process is described in detail, through to preliminary testing performed on the apparatus. The results obtained from the testing are analysed to determine whether they support the theoretical model provided. Evaluation of the simulator is provided, including proposals for further development of the apparatus and suggestions for more extensive testing.

Results are obtained from testing that indicate the relationship between sheet load, tailing load and angle of rope contact is as predicted. An approximately uniform coefficient of kinetic friction between the rope tested and the winch drum is determined. Its value is 0.1533.

List of Notations

β	The angle of contact of the rope on the winch drum
μ_k	The coefficient of kinetic friction
μ_s	The coefficient of static friction
σ	Stress
σ_Y	Yield stress
A	Cross-sectional area
B	***Winch base diameter***
D	Winch drum diameter
D_d	Winch drum diameter
F_a	Applied force (on winch handle)
H	Winch height
I	Moment of inertia about the horizontal neutral axis
L	Height to bottom of winch drum
L_h	Winch handle length
M	Bending moment
N	***The normal reaction force***
T_1	Tailing load. The tension in the rope leaving the winch
T_2	Sheet load. The tension in the rope leading into the winch
y	Distance from the neutral axis

1 Introduction

Sailing yacht design is an incredibly complex and diverse subject. Many different engineering principles have to be employed to design and analyse the great variety of components necessary for a yacht to perform at its best. Harnessing the power of the wind and the ocean can generate enormous forces, and engineers and naval architects must carefully analyse even the smallest details of design to ensure optimum performance, as well as guaranteeing the safety of the crew and those on board.

1.1 The Sailing Winch

There are many different types of sailing winch available to the modern yachtsman, depending on the type of vessel and the particular requirement of the winching task. The traditional type of winch is effectively a single speed drum mounted on bearings and attached to the deck or mast of a boat. The sheet or halyard is wrapped around the drum. The drum has a ratchet system allowing the drum to rotate in one direction only. This enables the sheet or halyard to be taken in, easily but not let out without the rope having to slip around the drum. The frictional force provided between the rope and the drum reduces the amount of force the operator needs to use to hold the rope steady. A handle is used to rotate the drum, and the length of the winch handle affects the amount of leverage that exists to aid the operator.

Figure 1 shows a winch in operation being used to haul in a genoa sheet (the front sail on a yacht)

Figure 1 *Genoa winch*

This is actually a self-tailing winch, which grips the free end of the rope to maintain the friction between the rope and the winch drum.

1.2 Types of Winch

Standard One, Two and Three Speed Winches[1]

These are the most basic sailing winches available on the market today. Figure 2 shows two different standard winches. The handle is wound clockwise for a 1:1 gear ratio. The handle of a two-speed winch can also be turned anti-clockwise to reduce the gear ratio and allow a greater torque to be produced at the winch surface for the same amount of operator's effort.

The operator must also provide a tailing load to maintain friction between the rope and the drum, thus prevent the winch from simply rotating under the sheet or halyard when wound.

Self-Tailing Winches

Self-tailing winches are a relatively modern development in winch technology. The free end of the rope is gripped at the top of winch drum, removing the requirement for the operator to provide a tailing load. Figure 3 shows examples of self-tailing winches

Other types of winches are available including electric and hydraulic self-tailing winches. These are more suited to larger boats with a higher budget.

1.3 Project Objective

The brief of this project is to design and construct a sailing winch simulator that is able to analyse the forces involved during the use of a sailing winch. Figure 2 shows the three basic force input and outputs involved with the usage of a standard winch

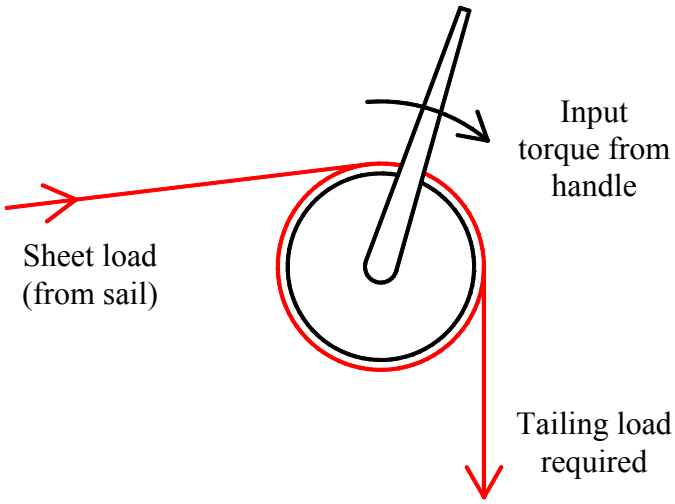

Figure 2 *Forces on a standard winch*

It is the intention of the project to investigate the relationship between the sheet load and the tailing as the number of turns around the winch (angle of contact between the rope and drum). There are a number of variables that might affect the relationship between loads. These are

- The age/condition of the rope
- Whether the rope is wet or dry
- The type of rope
- The surface finish of the winch drum
- The rope material
- The rope geometry

The sailing winch simulator should have the facility to study the affect of any, or all of these variables.

2 Theoretical Analysis

2.1 Friction of Rope Around a Drum

The basic fundamentals that are being investigated are the slippage, or impending slippage of rope, or a flexible belt around a drum. The tensions of the rope entering and exiting the drum can be analysed from first principles[2].

2.2 The Capstan Friction Equation

In this project, the frictional effects of rope around a sailing winch are being investigated. Figure 3 shows a rope slipping around a fixed drum.

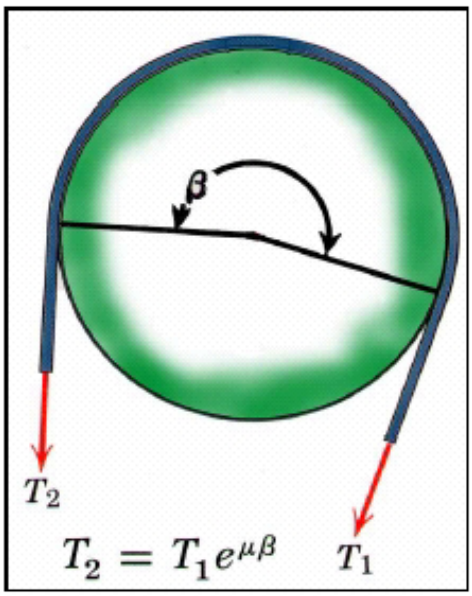

Figure 3 *The Capstan Friction Equation*

It can be proven that

$$T_2 = T_1 e^{\mu\beta} \qquad \text{(Eq}^{\text{n}}\text{ 1)}$$

Where β is the total angle of contact between the rope and the drum, expressed in radians and μ is the coefficient of friction, a dimensionless constant.

Figure 3 is a summary of the capstan friction equation for the friction of rope around a drum[3]. The capstan equation states that the frictional forces for slippage, or impending slippage of a rope around a drum depend on three things:

- The tension in the rope
- The coefficient of friction between the rope and the drum
- The total angle of contact between the rope and the drum

It should be noted that the frictional force is independent of contact area, and is also therefore independent of drum radius and the size of the rope.

For most cases it has been shown experimentally when load is increased up to impending motion, the coefficient of friction at the point of impending motion, i.e. when the frictional force is a maximum is generally higher than when slippage between the same to contacting surfaces is occurring. Hence, there usually exist two different coefficients of friction:

- The coefficient of static friction, μ_s, and
- The coefficient of kinetic friction, μ_k

For most cases, $\mu_s > \mu_k$.

3 Rig Design

The general specification for the sailing simulator is as follows, the rig must

- Support a winch with its rotational axis in the horizontal plane
- Have a fixing point for the sheet end of the rope
- Enable mass to be attached to the tailing end
- Internally support the loads produced by the winching process
- Have the facility to measure the tension in the sheet
- Enable different rope angles to be measured
- Enable different winches to be easily attached to the simulator

3.1 The Basic Form of the Rig

It was decided that the main section of the rig should have the basic form as shown in figure 4, which is an elevation of the rig

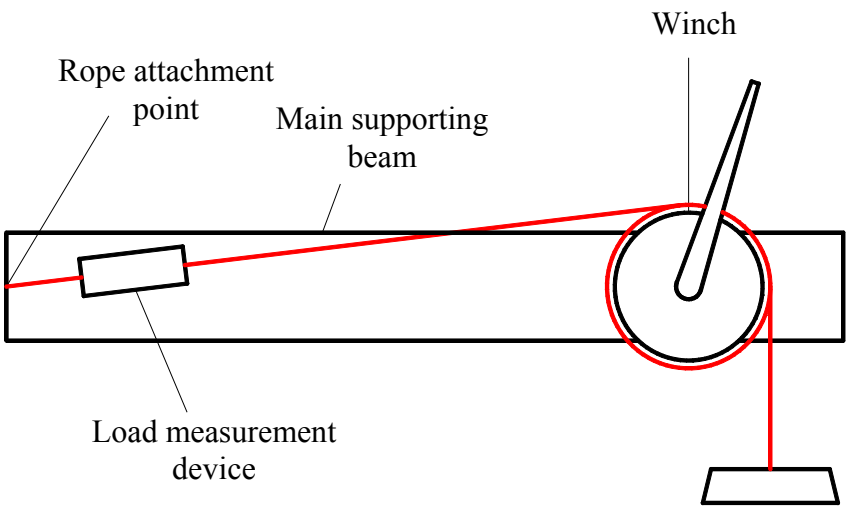

Figure 4 *Basic rig format*

This main rig section could then be reoriented to provide different numbers of turns of rope around the winch drum. By rotating the rig through 90° steps, for example, it would be possible to take measurements in ¼ turn steps.

The main supporting beam would carry the majority of the load created by the winching process. The simulator would carry the entire sheet load internally; the only force that would be transferred to the surroundings would be the weight of the rig itself, including the masses used to simulate the tailing load.

3.2 Detailed Rig Design

3.2.1 The Loads Involved

The first stage in the detailed rig design is to determine the forces that will be involved. It was important that a rig was designed that is capable of safely carrying the large loads that will be produced in the winching process.

3.2.2 Power Ratio

The power ratio[4] is the ratio of the sheet load, T_2, produced to the applied force, F_a, when no slippage occurs, and is defined as

$$PowerRatio = \frac{2L_h \times GearRatio}{D_d} \qquad \text{(Eq}^{\text{n}}\text{ 2)}$$

The power ratio for the winch that will be used is equal to 32:1.

For the purpose of designing the sailing winch simulator for measuring loads in the rope around a winch, it was said that the operator at 85kg putting their bodyweight onto the winch handle would cause the maximum force applied at the end of the handle.

By multiplying the maximum applied force by the power ratio, the maximum possible sheet load can be calculated, and is equal to

$$\text{Max. sheet load} = T_{2\max} = 9.81 \times 85 \times 32 = 26683.2N$$

The maximum force that the beam will have to support will be 26.7kN. This is a considerable load, and the design of the rig had to be carefully considered to ensure that it could support that amount of load.

3.2.3 The Winch

A Gibb 28 winch was kindly donated to the project. Although this winch was ceased and required stripping down, degreasing, and even machining to get it to run again, it was deemed beneficial to have a winch that could be tested to destruction if necessary to evaluate the effectiveness of the rig. The dimensions of the winch are shown in

H = 140mm

D = 76mm

L = 65mm

B = 115mm

3.2.4 Main Supporting Beam

It was decided the most economical method for manufacturing the rig, both in terms of cost and time, would be to examine the available steelwork within the department, and see if any would be suitable for manufacturing the main steelwork of the rig. The first component to be sourced was the main supporting beam.

The smallest available beam section available within the department long enough to form the main supporting beam, was an RSJ 158x77x9mm. It was evaluated to see if it would be suitable for the task.

It should be noted that the maximum force, T_{2max}, is offset from the surface of the beam by 65mm, due distance from the bottom of the winch to the base of the drum. The distance of 144mm is the perpendicular distance from the force to the neutral axis of the beam.

To calculate the maximum stress in the beam, Engineer's Theory of Bending is used. The stress, σ, at any point in the beam is calculated using the formula

$$\sigma = \frac{My}{I} \qquad \text{(Eq}^{\text{n}}\text{ 3)}$$

Where M = bending moment applied (Nm), y = distance from the neutral axis evaluated (m), I = moment of inertia about the horizontal neutral axis (m^4).

The maximum stress, σ_{max} = 33.45 MPa

The yield stress for mild steel is 290 MPa, hence the maximum stress that the beam can possibly observe is only 11.5% yield. From this it is clear the RSJ available will be strong enough to support the loads involved with a large factor of safety. This means the main supporting beam is over-engineered, but it was deemed better to utilise the resources already available than order in a lighter, weaker beam for the reasons previously outlined.

4 Load Measurement System

4.1 Choice of Load Measurement System

It was required that the sheet load be measured by a suitable device in order to determine the effect of a number of different variables on the relationship between the sheet load, the tailing load, and the angle of contact of the rope around the drum. It was determined that the load cell would sit in series with the sheet, and would measure the tension in the rope.

4.2 Load Cell Design

4.2.1 Specification

The method for calculating the maximum sheet load has been detailed in section 3.2.2, and is given by

$$\text{Max. sheet load} = T_{2\max} = 9.81 \times 85 \times 32 = 26683.2N$$

4.2.2 Specimen Design

The yield stress, σ_Y, for the steel used 540 MPa[5]. The stress that the maximum sheet load should produce is ½ σ_Y = 270 MPa.

During uniaxial loading in a bar of uniform cross-sectional area, stress, σ, is equal to the force divided by the cross-sectional area, A.

$$\sigma = \frac{F}{A} \qquad \text{(Eq}^{\text{n}}\text{ 4)}$$

To determine the cross-sectional area of the specimen, the equation is solved for ½ σ_Y and $T_{2\max}$

$$A = \frac{T_{2\max}}{1/2\sigma_Y} \qquad \text{(Eq}^{\text{n}}\text{ 5)}$$

Eq^{n} 20 solves to give a cross-sectional area of 9.883×10^{-5} m^2.

By using square steel bar

$$b = \sqrt{A} \qquad \text{(Eq}^{n}\text{ 6)}$$

This gives a value of b = 9.94mm. Square section steel bar of 10mm x 10mm was used for the load cell specimen.

Strain gauges were bonded to the specimen and connected to a Wheatstone bridge configuration to eliminate bending effects and compensate for thermal expansion.

Figure 5 shows the load cell in its position in the rig

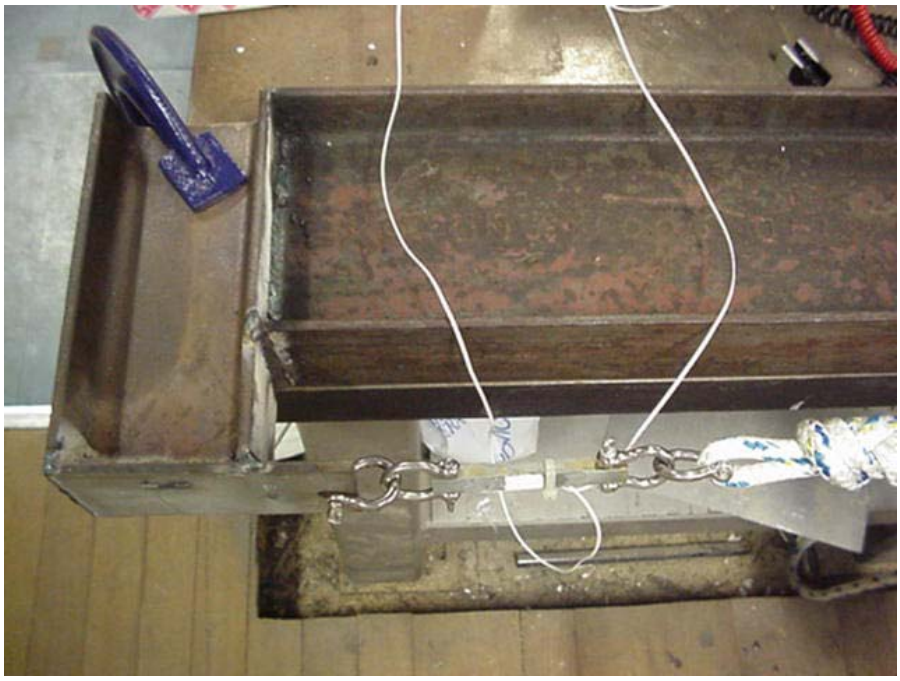

Figure 5 *Load cell in position*

4.2.3 Calibration

A 5V power supply was connected to supply an excitation voltage across the stain gauges. A sensitive voltmeter measuring mV was connected to measure the signal voltage. Figure 31 shows the power supply and the voltmeter

The load cell was connected into the tensile testing machine. The variables measured were the load applied (tension in kN), and the voltage change across the strain gauges (mV). It should be noted that the voltmeter was 'zeroed' when the force was removed from the load cell; the change in voltage was read directly from the voltmeter.

It is standard practice to load and unload a load cell a number of times during calibration to ensure that all the bonds between the strain gauges and the load cell specimen settle. This process is known as 'scragging'.

Figure 6 shows a chart of average change in voltage output against applied load

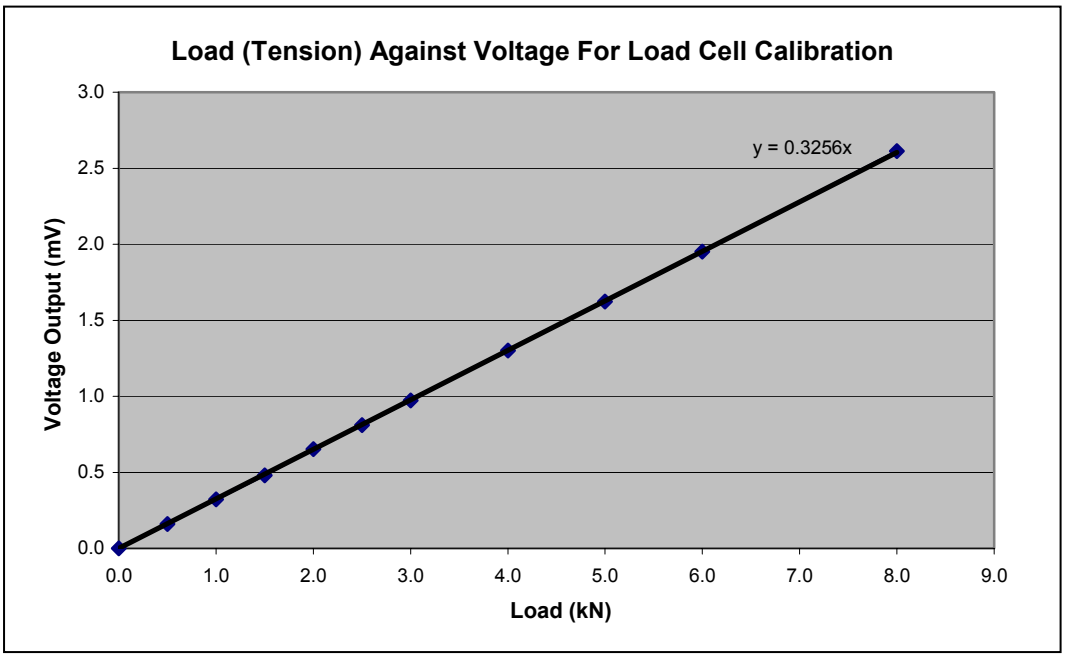

Figure 6 *Load cell calibration results*

The calibration results indicate that the load cell has excellent linearity. By plotting a linear regression trendline through the results and displaying the equation on the chart, it is easy to see that a conversion between change in voltage and load can be

easily calculated, simply by multiplying the voltage value read from the voltmeter in mV by 0.3256 to give the load that the load cell is experiencing in kN.

5 The Completed Rig

Figure 7 shows a photograph of the complete rig in place and ready for testing.

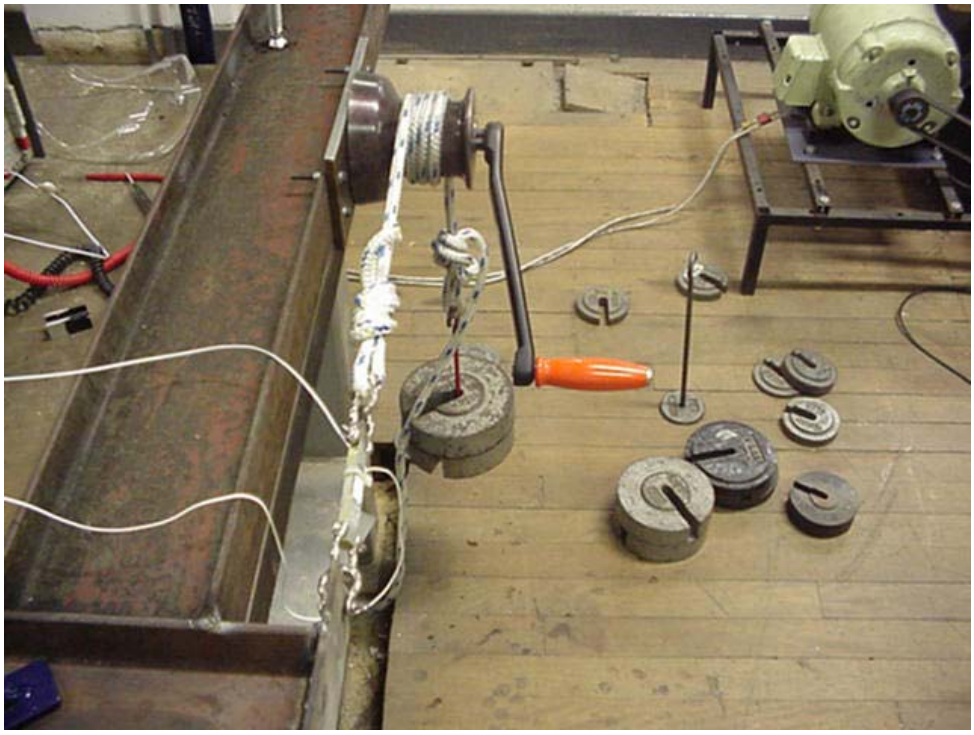

Figure 7 *The completed rig ready for testing*

6 Testing Procedure

6.1 Broad Aims

The brief for the project is to design and construct a sailing winch simulator. It has never been the aim to carry out extensive testing of the effect of different variables such as the age or type of rope, whether the rope is wet or dry etc. (these variables have been discussed previously). It is, however, important to ensure that the system as a whole is successful in producing meaningful and accurate results that can be analysed.

For each number of turns, the tailing load was varied over a realistic range, and the sheet load was measured using the load cell. As many different combinations of turn numbers as possible around the winch would be tested.

The rig was firmly attached with G-clamps to a solid workbench, which was itself already bolted to the floor.

6.2 Load Measurement

For each different rope angle tested, the tailing load was the variable that was controlled. The sheet load was measured using the load cell produced at an earlier stage in the project. A voltage output from the strain gauges attached to the load cell was given in mV from a sensitive voltmeter, where the change in voltage is directly proportional to the load applied to it (axial tension).

6.3 Testing Procedure Overview

1. Rig clamped horizontally to workbench.
2. Set up with ¼ turn of rope around drum.
3. Voltmeter 'zeroed' when load cell is unloaded.
4. Mass hanger tied to loop in vertically hanging free end of rope.
5. Winch handle rotated so that rope is slipping over drum.
6. Voltage read from voltmeter and noted.
7. Load released and voltmeter 'zeroed' when load cell is unloaded (if necessary)
8. Steps 4 to 7 repeated until a total of 5 voltage readings are obtained for initial tailing load.
9. Tailing load increased and steps 3 to 8 repeated until slippage cannot be obtained by manually turning the handle.
10. The rope angle is increased by one complete turn and steps 3 to 9 repeated until all rope angles for the rig orientation are tested
11. Rig rotated 180° and steps 1 to 10 repeated (starting with ¾ turn and increasing to 3 ¾ turns).

This gave an array of results for a total of nine different rope angles, ranging from a ¼ turn up to 4 ¼ turns in ½ turn steps.

6.4 Analysis of Results

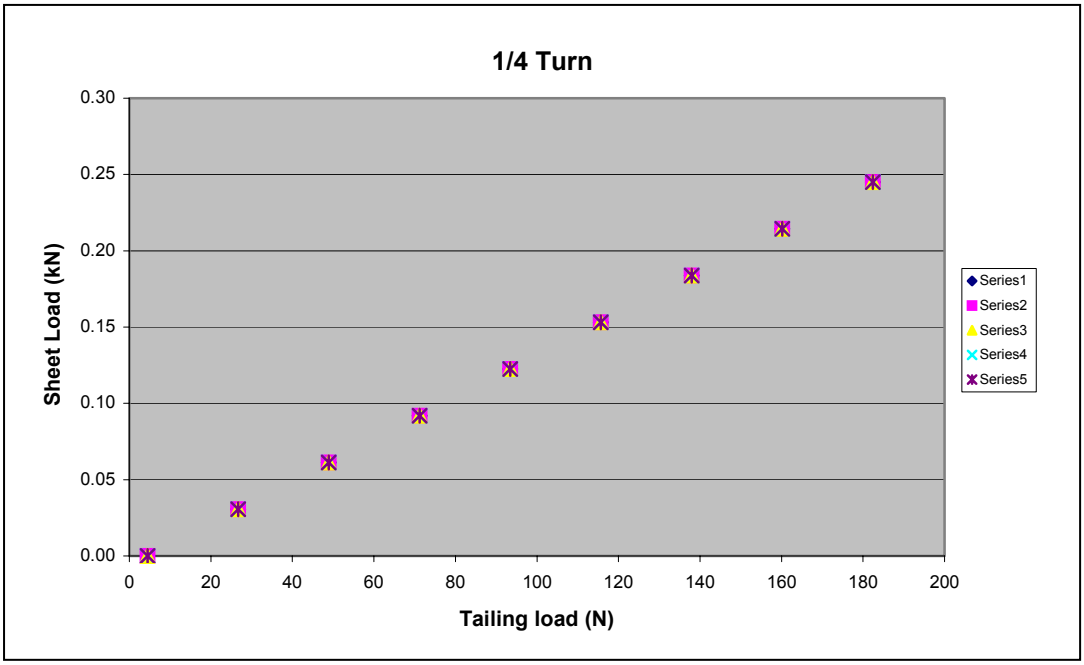

Figure 8 *Variation of sheet load with tailing load for ¼ turn*

Figure 8 shows this chart for a ¼ turn. All the data series coincide. Closer inspection of the test data shows that for each tailing load applied, the same voltage was recorded for the initial and four repeat readings. This is due to sensitivity of the load cell. It was necessary when designing the load cell to sacrifice some low-end sensitivity in order to obtain a sufficient range to allow the largest possible loads obtained during testing to remain in the linear stress-strain range of the load cell. The five coincident points on the chart for each value of tailing load does also indicate that this rope angle at least, the test is very repeatable. The relationship is clearly linear.

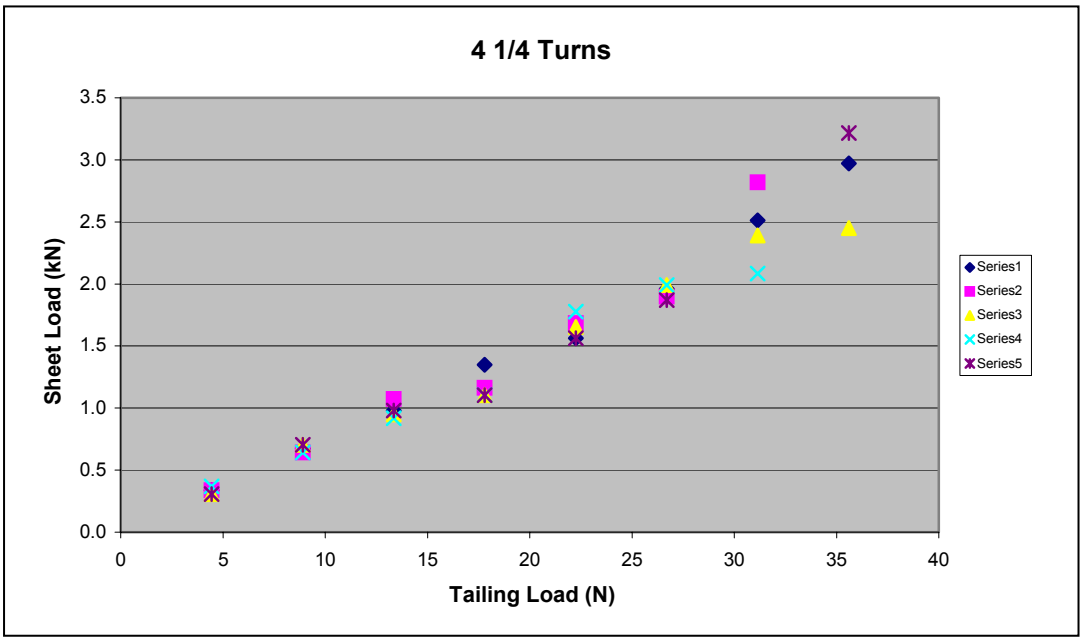

Figure 9 *Variation of sheet load with tailing load for 4 ¼ turns*

Figures 8 and 9 show results arrays for a ¼ turn and 4 ¼ turns respectively. These two are picked because they are at the two extremities of rope angle. It is evident from the testing that the amount of scatter in the data increases with the rope angle, or more accurately, the sheet load. It is expected that the sheet load would vary linearly with tailing load. Recall the relationship:

$$T_2 = T_1 e^{\mu\beta} \qquad \text{(Eq}^{\text{n}}\text{ 1)}$$

Rearranging gives:

$$\frac{T_2}{T_1} = e^{\mu\beta} \qquad \text{(Eq}^{\text{n}}\text{ 2)}$$

For each rope angle tested, the exponential function on the right hand side of eq^{n} 2 is constant as the rope angle, β, and the coefficient of friction between the rope and the drum, μ, are constant and do not vary with either forces. Hence T_2/T_1 should be a constant, and this is demonstrated to be so by the linear relationships between the two forces, which are shown on the charts of all angles tested. The gradient of the graphs should therefore, according to the theory being testing, be equal to the exponential function, $e^{\mu\beta}$.

By plotting the average sheet load against tailing load for all the angles tested on one chart, the full array of results can be viewed simultaneously. Figure 10 shows all these.

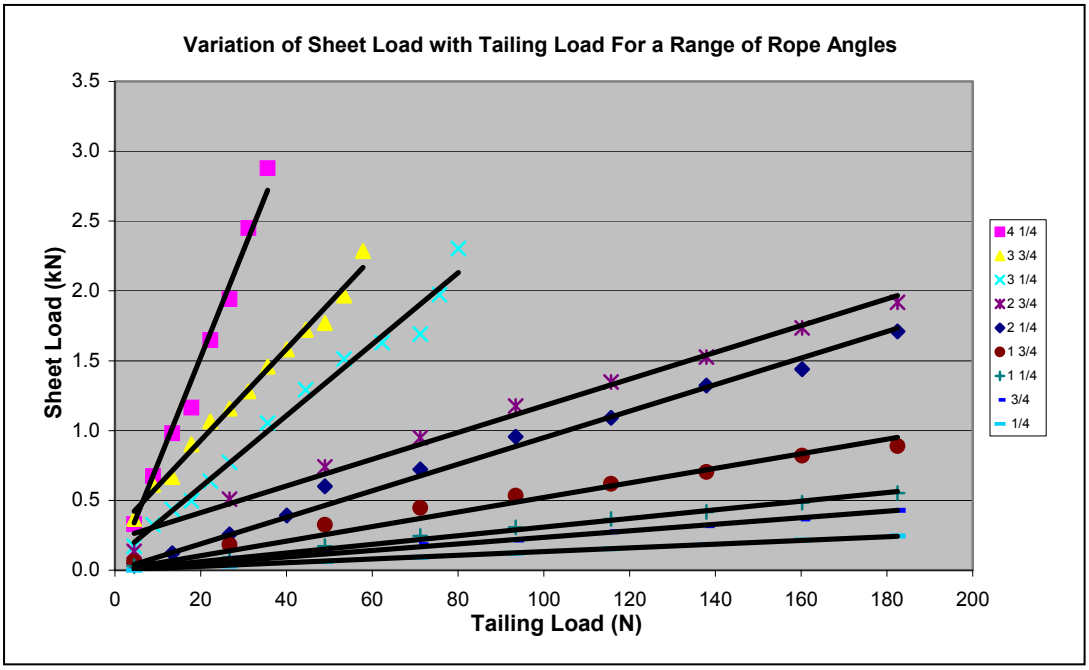

Figure 10 *Variation of Sheet Load with Tailing Load For a Range of Rope Angles*

Linear regression trendlines have been added to all the data series. This gives a better demonstration the linearity of the relationship. Microsoft excel provides the function of displaying the equation of the linear regression trendline on the chart itself, enabling the gradient to be easily obtained for each rope angle tested. The equations have been omitted from figure 10 for clarity, but table 1 shows the rope angles and corresponding gradients.

Rope Angle		Gradient	Log_e(Gradient)
No. of Turns	Radians		
¼	π/2	1.3	0.26
¾	3π/2	2.4	0.88
1 ¼	5π/2	3.1	1.13
1 ¾	7π/2	5.2	1.65
2 ¼	9π/2	9.5	2.25
2 ¾	11π/2	9.6	2.26
3 ¼	13π/2	25.6	3.24
3 ¾	15π/2	32.7	3.49
4 ¼	17π/2	76.4	4.34

Table 1 *Gradients of trendlines taken from chart in figure 44*

Also given in table 3 are the natural logs of each of the gradients. If eq^n 2 is further manipulated, it can be shown to give:

$$Log_e\left(\frac{T_2}{T_1}\right) = \mu \cdot \beta \qquad \text{(Eq}^n\text{ 3)}$$

Hence, by plotting the natural log of the gradients against the rope angle, the resulting gradient should give the frictional coefficient between the rope and the winch drum (whether a straight line or a function of angle). Figure 11 shows this plot.

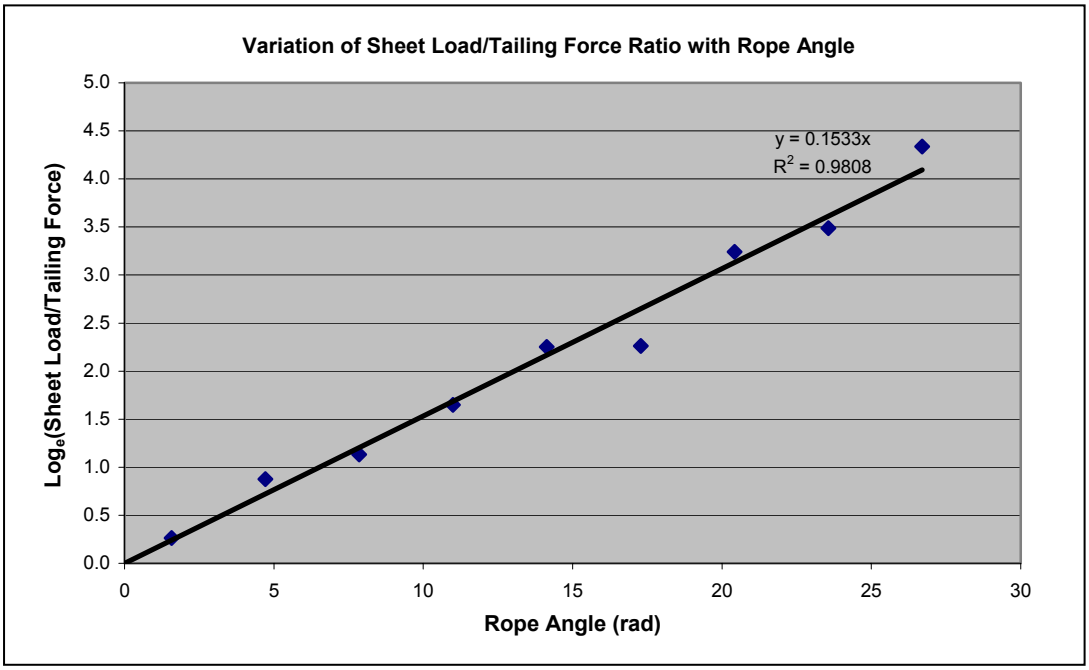

Figure 11 *Variation of natural log of gradients with rope angle*

A linear relationship has been shown between the natural logs of the gradients of the sheet load-tailing load graphs and the rope angle. This shows that the winch appears to behave in the way predicted by the theory. A linear regression trendline can be drawn through the data, which passes through the origin. The equation of the trendline marked on the chart, showing that the gradient of this line is constant and has a value of 0.1533. It can be deduced from the theory that the coefficient of kinetic friction, μ_k, between the rope used and the surface of the winch drum on the test rig has a constant value of 0.1533. Microsoft Excel also has the facility of calculating the R^2 value of the correlation. This is a measure how successful the linear regression is at explaining the response. R^2 gives us the variance of the predicted responses as a fraction of the variance of the actual responses[6]. In this case R^2=0.9808. This means that the linear relationship will explain 98.1% of the variation in the natural log of the sheet load to tailing load ratios. This gives an indication that the linear relationship is strong and can be relied on.

A possible reason for the small deviation from the linear relationship could be that the rope became worn towards the end of the testing period, causing the coefficient of friction to reduce. It should be noted that the results below the trendline were taken later in the testing programme. It is also possible that inconsistent surface finish on the winch drum may cause irregularity.

6.5 Torque Measurement

During the testing programme, a quick investigation into the amount of torque required to produce slippage was performed. This was a crude test, and the results of which should not be analysed too heavily, it was to demonstrate a measurement of the input torque could be taken.

A torque wrench was connected to the winch

The torque wrench could be set to a given torque value, and if this torque was exceeded, then the wrench would click to signal the operator. For 4 ¼ turns, two tailing loads were tested, and the torque value was gradually induced until slippage occurred. The results are shown in table 2

Tailing Load (N)	Torque (Nm)	Calculated Sheet Load (kN)	Ave. Measured sheet load (kN)
13.4	51.5	1.36	0.98
17.8	71.3	1.87	1.16

Table 2 *Torque results*

The sheet load that appears to be induced by the torque wrench is similar to that measured by the load cell. It was not expected to be exactly the same, it is, however, encouraging that the results are of the same order, and the torque measurement could be investigated further.

7 Evaluation

7.1 Success of Testing

A full set of results over the full operating range of the winch was obtained. Rope angles measuring from a ¼ turn up to 4 ¼ turns were tested. The results enabled theory to be tested, and to a certain extend the results appeared to compound the theory. In this respect, the testing procedure was a success.

7.2 Extension to the Project

A number of issues arose when reviewing the results from testing. A number of possible areas of development or extension to the project exist.

- Data Acquisition.

  A data acquisition system that would perhaps log the sheet load time history would demonstrate the sheet load increases as the winch is wound. The testing procedure followed measured the forces during kinetic friction, i.e. during slippage. This would enable static friction to be analysed, characteristics such as peak sheet load to be measured

- The effect of other variables

  It would be important to test the effect of rope variables on the results. The age of the rope, whether the rope is wet or dry, the type of rope, and the dimensions of rope are all variables that might be investigated. These might affect the coefficient of friction

- Investigating different winch types

There are any number of different types of winches available, with different dimensions, gearing ratios, drum surface finishes etc. Investigations into how different winches perform, or a comparison between different types of winches could prove to be a worthwhile study. A cylinder with a uniform surface finish may be a good starting point in evaluating practical application of the capstan friction equation.

- Torque measurement

  A quick and crude torque measurement investigation was carried out. However, this provided far from conclusive results. By developing a system for accurately measuring the input torque, an investigation into the internal friction of the winch could perhaps be performed. Perhaps data acquisition would be useful here also.

7.3 Project Conclusion

Overall the project has been a success. The results obtained from testing have proven the sailing winch simulator designed and manufactured can produce meaningful results that can be used to analyse the forces concerned with sailing winch operation. The results do not wholly support the theory discussed, but the reasons for this have been considered, and further testing has been proposed evaluate this more extensively. A distinct design process was followed which led to the production of a functional sailing winch simulator.

7 Acknowledgements

The author would like to thank Dr McLaren, who always made himself available to provide advice and encouragement throughout the course of the porject, and seemed to consistently suggest practical solutions that made the weekly tasks seem far less daunting. Many thanks also go to the technicians, particularly to Chris Cameron, Andy Crockett and Willie Mason, who gave up their time to offer advice and practical expertise.

8 References

[1] Figures 2 and 3 taken from http://www.lewmar.com/webcat/index.asp
[2] Meriam, J.L., Kraige, L.G., Engineering Mechanics Volume One: Statics, Second Edition, Jonh Wiley and Sons, Chap. 6/8.
[3] Attaway, S.W., The Mechanics of Friction in Rope Rescue, International Technical Rescue Symposium 1999
[4] http://www.boatus.com/boattech/winches.htm
[5] RS Data Pack G, Engineering Materials, 1997
[6] Moore, D.S.,McCabe,G.P., Introduction to the Practice of Statistics 3rd Edition, W.H. Freeman and Company, New York, Chap. 2.3.